

Transport in periodic potentials induced by fractional Gaussian noise

Bao-quan Ai¹, Ya-feng He², and Wei-rong Zhong³

¹*Laboratory of Quantum Information Technology, ICMP and SPTE,
South China Normal University, 510006 Guangzhou, China.*

²*College of Physics Science and Technology,
Hebei University, 071002 Baoding, China.*

³*Department of Physics, College of Science and Engineering,
Jinan University, 510632 Guangzhou, China.*

(Dated: October 6, 2018)

Abstract

Directed transport of overdamped Brownian particles driven by fractional Gaussian noises is investigated in asymmetrically periodic potentials. By using Langevin dynamics simulations, we find that rectified currents occur in the absence of any external driving forces. Unlike white Gaussian noises, fractional Gaussian noises can break thermodynamical equilibrium and induce directed transport. Remarkably, the average velocity for persistent fractional noise is opposite to that for anti-persistent fractional noise. The velocity increases monotonically with Hurst exponent for the persistent case, whereas there exists an optimal value of Hurst exponent at which the velocity takes its maximal value for the anti-persistent case.

PACS numbers: 05. 40. Fb, 02. 50. Ey, 05. 40. -a

Keywords: Ratchet, fractional Brownian motion

I. INTRODUCTION

In systems possessing spatial or dynamical symmetry breaking, Brownian motion combined with unbiased external input signals, deterministic or random alike, can assist directed motion of particles in nanoscale systems[1]. The subject of the fluctuation-induced transport was motivated by the challenge to explain unidirectional transport in biological systems[2], as well as their potential technological applications ranging from classical non-equilibrium models[3] to quantum systems[4]. Ratchets have been proposed to model the unidirectional motion driven by zero-mean non-equilibrium fluctuations. Broadly speaking, ratchet devices fall into three categories depending on how the applied perturbation couples to the substrate asymmetry: rocking ratchets[5], flashing ratchets[6], and correlation ratchets [7]. Additionally, entropic ratchets, in which Brownian particles move in a confined structure, instead of a potential, were also extensively studied [8].

Anomalous diffusion has attracted growing attention, being observed in various fields of physics and related sciences [9], where by contrast with Brownian motion, long-range temporal correlations induce nonstandard dynamical behaviors. The diffusion is characterized through the power law form of the mean-square displacement $\langle x^2(t) \rangle \propto t^\alpha$. According to the value of the index α , one can distinguish subdiffusion ($0 < \alpha < 1$), normal diffusion ($\alpha = 1$) and superdiffusion ($\alpha > 1$). In the literature, two popular stochastic models have been used to account for anomalous diffusion. The first model is the continuous-time random walk [9–14]. In this model, the subdiffusion is caused by the long waiting time between successive jumps and the superdiffusion is induced by the long jumps. In the minimal Lévy ratchet[10–14], the heavy-tailed distribution of the α -stable noise can break the thermodynamical equilibrium and induce directed transport.

The second model is fractional Brownian motion (FBM) introduced by Mandelbrot and Van Ness [15]. FBM has wide applications in some complex systems, such as monomer diffusion in a polymer chain [16], diffusion of biopolymers in the crowded environment [17], single file diffusion [18], and translocation of the polymer passing through a pore [19]. The statistical properties of FBM are characterized by the Hurst exponent $0 < H < 1$. In particular, its meansquared displacement satisfies $\langle x^2(t) \rangle \propto t^{2H}$, thus for $H < 1/2$ one can obtain the subdiffusive dynamics, whereas for $H > 1/2$ the superdiffusive one [20]. In the last few years, there has been a growing interest in the study of the FBM [21–24]. However,

most studies of FBM focus on the free FBM and a few studies on FBM have been involved the potentials. Recently, Sliusarenko and coworkers [25] studied the escape from a potential well driven by fractional Gaussian noises and found that the escape becomes faster for decreasing values of Hurst exponent. Chaudhury and Cherayila [26] studied the first passage time distribution for barrier crossing in a double well under fractional Gaussian noises. It is uncertain whether fractional Gaussian noise can induce directed transport in the absence of any external driving forces. In order to answer this question, we studied the transport of overdamped Brownian particles driven by fractional Gaussian noises in asymmetrically periodic potentials. We focus on finding the rectified mechanism and how noise intensity and Hurst exponent affect the transport.

II. MODEL AND METHODS

In this study, we consider the directed transport of the Brownian particles driven by fractional Gaussian noises in the absence of whatever additional time-dependent forces. The overdamped dynamics can be described by the following Langevin equation in the dimensionless form

$$\eta \frac{dx}{dt} = -U'(x) + \sqrt{\eta k_B T} \xi_H(t), \quad (1)$$

where $\xi_H(t)$ is the fractional Gaussian noise, $D = \frac{k_B T}{\eta}$ is noise intensity, and H is the Hurst exponent. η is the friction coefficient of the particle, k_B is the Boltzmann constant, and T is the absolute temperature. The prime stands for differentiation over x . $U(x)$ is an asymmetrically periodic potential

$$U(x) = -U_0 \left[\sin(x) + \frac{\Delta}{4} \sin(2x) \right], \quad (2)$$

where U_0 denotes the height of the potential and Δ is its asymmetric parameter.

Fractional Gaussian noise is a zero mean stationary random process with long memory effects [21–25]. It is closely related to the FBM process [27], which is defined as a Gaussian process with an exponent $0 < H < 1$ and

$$\langle \xi_H(t) \rangle = 0, \quad (3)$$

$$\langle \xi_H(t) \xi_H(s) \rangle = \frac{1}{2} [t^{2H} + s^{2H} - (t-s)^{2H}], \quad (4)$$

for $0 < s \leq t$. In the long time limit, the autocorrelation function will decay as

$$\langle \xi_H(0)\xi_H(t) \rangle \propto 2H(2H - 1)t^{2H-2}, \quad (5)$$

for $0 < H < 1$ and $H \neq \frac{1}{2}$. When $H = \frac{1}{2}$, fractional Gaussian noise reduces to white Gaussian noise. From Eq. (5), it is easy to find that the noises are positively correlated (persistent case) for $\frac{1}{2} < H < 1$, and negatively correlated (anti-persistent case) for $0 < H < \frac{1}{2}$.

Though FBM is an old topic, the consistent analytical methods are still not available. Here we will study the transport of the Brownian particles by using Langevin dynamics simulations. From Eqs. (1) and (4) one can obtain the discrete time representation of Eq. (1) for sufficiently small time step δt

$$x(t_{n+1}) = x(t_n) - U'(x(t_n))\delta t + \sqrt{D}\delta t^H \xi_H(n), \quad (6)$$

where $n = 0, 1, 2, \dots$ and $\xi_H(n)$ is fractional Gaussian random number. We used the method described in [25, 28, 29] for simulating fractional Gaussian random number.

In this study, we mainly focus on the transport of the driven particles. The average velocity v is used to measure the transport,

$$v(t) = \frac{1}{N} \sum_{i=1}^N \frac{x_i(t) - x_i(t_0)}{t - t_0}, \quad (7)$$

where N is the number of the realizations and t_0 and t are the initial and the end time for the simulations, respectively. The asymptotic velocity V is

$$V = \lim_{t \rightarrow \infty} v(t). \quad (8)$$

III. NUMERICAL RESULTS AND DISCUSSION

In order to check the convergence of the algorithm, we have studied the dependence of average velocity on time step δt , the end time t , and the number N of the realizations. From Fig. 1(a), (b) and (c), we can see that the algorithm is convergent and the numerical results do not depend on the calculation parameters (δt , t , and N) when $\delta t < 10^{-3}$, $t > 10^4$, and $N > 10^4$. Therefore, in our simulations, the number of the realizations is more than 4×10^4 realizations, time step is chosen to be smaller than 10^{-3} and $t = 10^4$. Fig. 1(d) shows the estimated relative errors as a function of the noise intensity D at $N = 4 \times 10^4$, $t = 10^4$, and

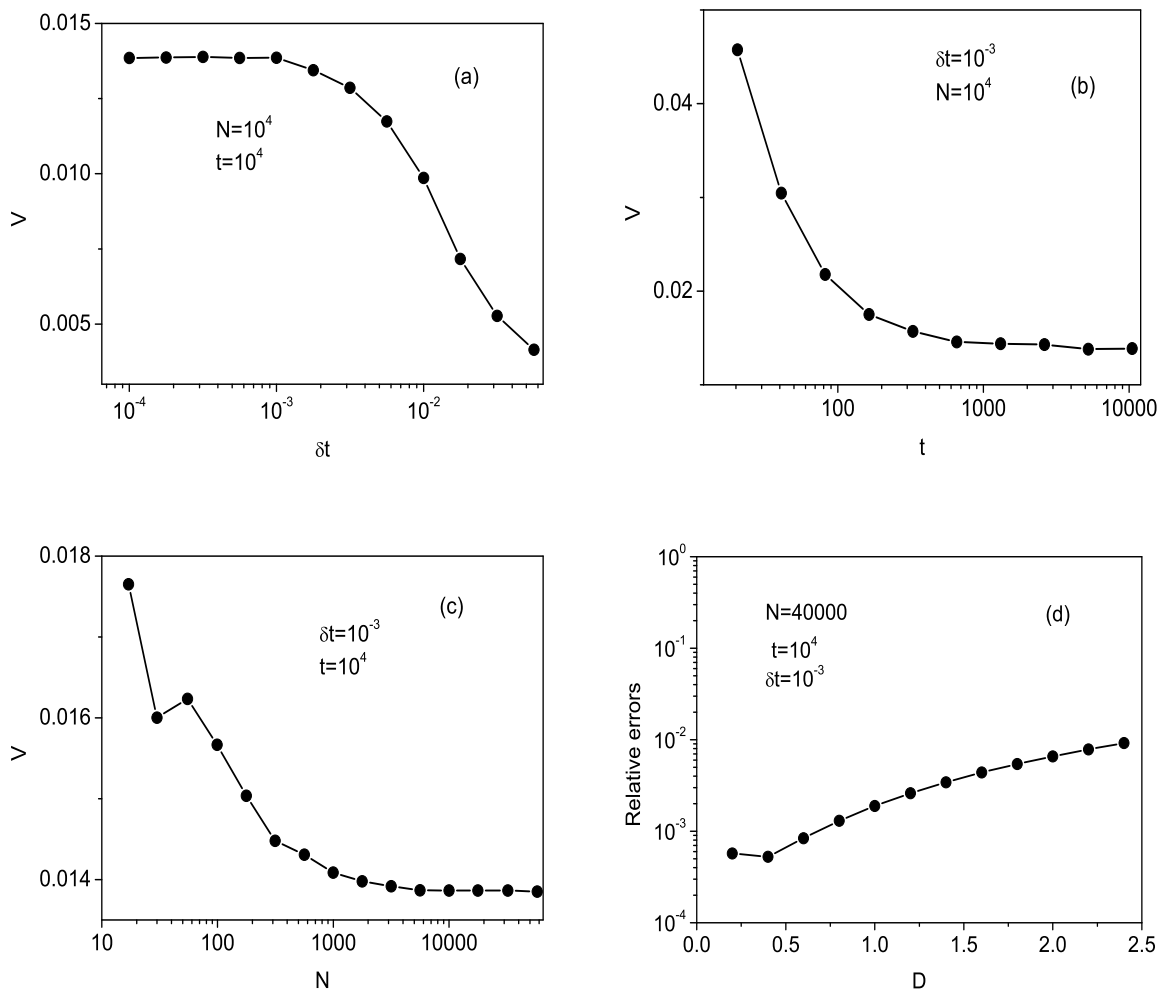


FIG. 1: Convergence and relative errors of the algorithm. (a) Dependence of V on time step δt at $N = 10^4$ and $t = 10^4$; (b) dependence of V on the end time t for simulations at $\delta t = 10^{-3}$ and $N = 10^4$; (c) dependence of V on the number N of the realizations at $\delta t = 10^{-3}$ and $t = 10^4$; (d) dependence of estimated relative errors on noise intensity D . The other parameters are $D = 0.5$, $U_0 = 1.0$, and $\Delta = 1.0$.

$\delta t = 10^{-3}$. It is found that the relative errors are less than 0.01 even for large values of the noise intensity. Therefore, the parameter we used are sufficient to obtain consistent results.

First, we study the properties of FBM for both persistent and anti-persistent cases. Figure 2 shows the simulated sample paths for different values of H . The differences among these three cases are clear. For $H = 0.3$, the negative correlation accounts for high variability,

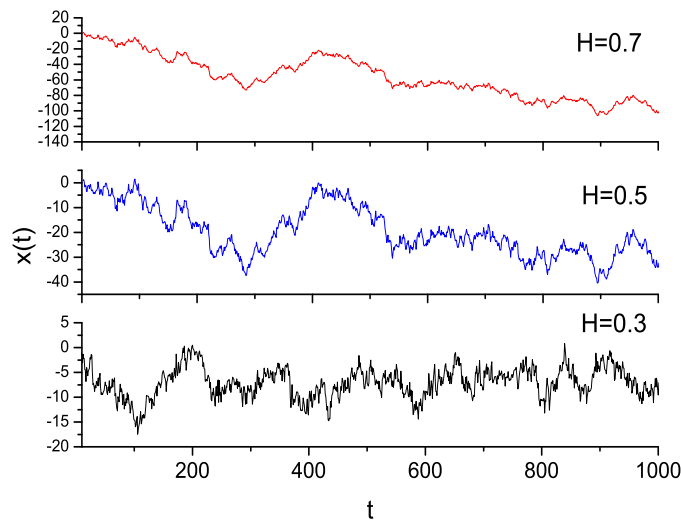


FIG. 2: (Color online) Samples of FBM for different values of the Hurst exponent $H = 0.3, 0.5,$ and 0.7 .

whereas the sample is more smooth for $H = 0.7$ due to the positive correlation [29].

The frequency spectrum of the external drive is very important to determine direction of motion of the Brownian particles in periodic potentials. In our minimal ratchet setup, fractional Gaussian noise is the only external drive, so it is necessary to analyze its frequency properties. In Fig. 3, we investigate the spectral density of fractional Gaussian noise for different values of H . We can find that the distributions of the frequency are different for the three cases. For white Gaussian noise ($H = 0.5$), the spectral density is uniform. However, the low frequency component is larger than the high frequency part in the spectral density for the persistent case ($H = 0.7$). For the anti-persistent case ($H = 0.3$), the high frequency component is larger in the spectral density. In order to facilitate the analysis of the driving mechanisms, persistent fractional Gaussian noise can be artificially divided into two frequency components: white Gaussian noise and low frequency ac drive. Similarly, the anti-persistent fractional Gaussian noise in frequency domain is equivalent to a compound of white Gaussian noise and high frequency drive.

Next, we will study the directed transport mechanism for our ratchet. Usually, the ratchet mechanism demands three key ingredients [1]: (a) nonlinear periodic potential, (b) asymmetry of the potential or external driving forces, and (c) fluctuating. Figure 4 (a)

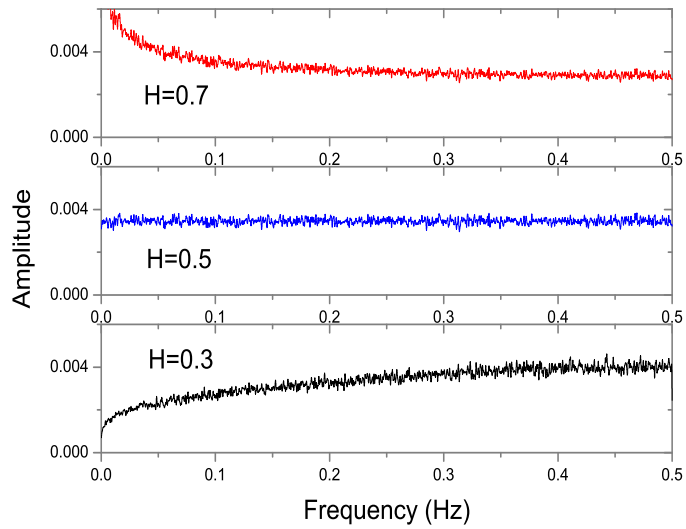


FIG. 3: (Color online) The spectral density of the noises for different values of Hurst exponent $H = 0.3, 0.5,$ and 0.7 .

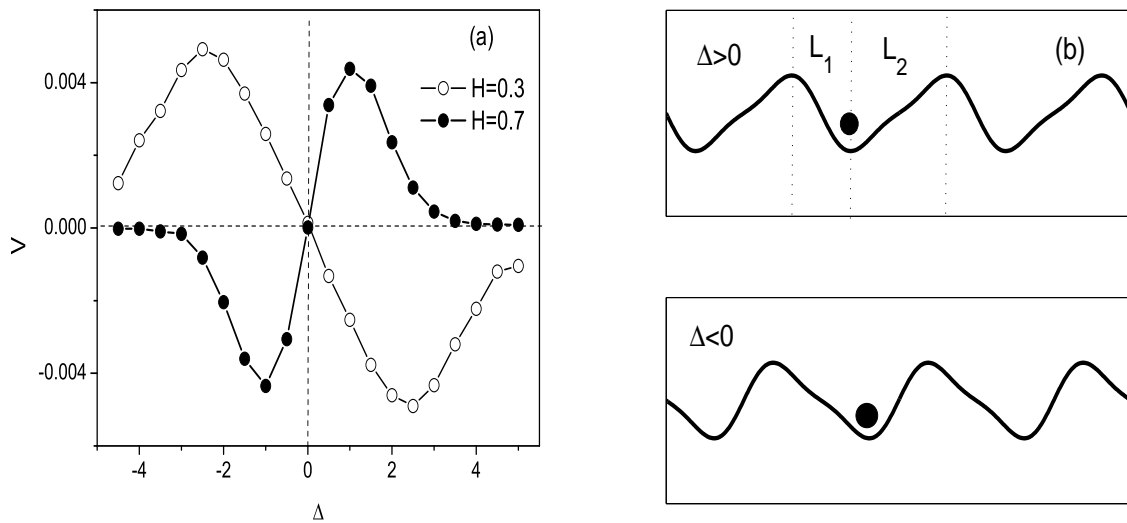


FIG. 4: (a) Average velocity v as a function of the asymmetric parameter Δ of the potential for both persistent and anti-persistent cases at $D = 0.3$ and $U_0 = 1$. (b) Asymmetrically periodic potential for $\Delta > 0$ and $\Delta < 0$, L_1 is the length from the minima of the potential to the maxima from the left side and L_2 is the length from the right side.

shows the average velocity as a function of the asymmetry of the potential. For the persistent case ($H = 0.7$), the velocity is positive for $\Delta > 0$, zero at $\Delta = 0$, and negative for $\Delta < 0$. However, for anti-persistent case one can obtain the opposite velocity, negative for $\Delta > 0$ and positive for $\Delta < 0$. Moreover, for both cases, there exists an optimal value of Δ at which the velocity takes its extremal value. When $\Delta \rightarrow 0$, the system is absolutely symmetric and directed transport disappears. When $\Delta \rightarrow \infty$, the asymmetric potential described in Eq. (2) reduces to symmetric one ($U(x) = -\frac{U_0}{4}\Delta \sin(2x)$) with higher barriers, resulting in zero velocity.

Now we will give the physical interpretation of the directed transport for the case of $\Delta = 1$ (see the upper of Fig. 4 (b)). We define three time periods that are very important for explanation of the directed transport: driving period T , diffusion time T_1 for crossing the steeper slope (the left side) from the minima, and diffusion time T_2 for crossing the gentler slope (the right side). Because of $L_1 < L_2$, T_1 is always less than T_2 . Firstly, the particles stay in the minima of the potential (see Fig. 4 (b)) until they are catapulted out of the well by a large amplitude fluctuation. For the persistent case ($H = 0.7$), the fractional Gaussian noise contains more low frequency components (see the upper of the Fig. 3) and it can be divided into two parts: white Gaussian noise and low frequency ac drive. Due to the low frequency, the drive has a very long period and $T \gg T_2 > T_1$. All particles get enough time to cross both sides from the minima of the potential before the drive reverses its direction. However, the left side is steeper than the right one, more particles climb the barrier from the right side, so the average velocity is positive. For the anti-persistent case ($H = 0.3$), the high frequency components dominate over the low frequency ones (see the bottom of the Fig. 3). In this case, the drive has a short period and $T_1 < T < T_2$ (or $T < T_1 < T_2$). In a short driving period, the particles have sufficient time to diffuse across the steeper side of the well, resulting in negative average velocity. It should be pointed out that the average velocity will tend to zero for the case of $T \ll T_1 < T_2$ (very small values of H) which is also shown in Fig. 6.

The noise intensity dependence of the average velocity is shown in Fig. 5 for different values of Hurst exponent. The curve is observed to be bell shaped. When $D \rightarrow 0$, the particles cannot pass across the barrier and there is no directed current. When $D \rightarrow \infty$ so that the noise is very large, the effect of the potential disappears and the average velocity tends to zero, also. Therefore, one can see that the curves demonstrate nonmonotonic

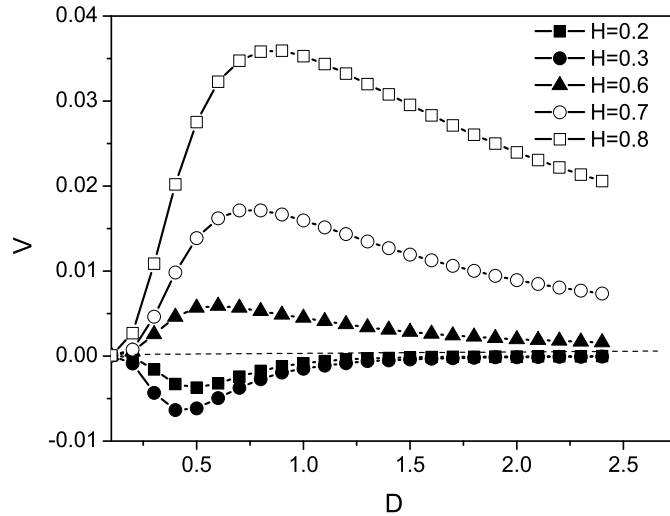


FIG. 5: Average velocity V as a function of noise intensity D for different values of Hurst exponent $H = 0.2, 0.3, 0.6, 0.7,$ and 0.8 at $\Delta = 1.0$ and $U_0 = 1$.

behavior.

Figure 6 displays the Hurst exponent dependence of the average velocity at $\Delta = 1.0$. It is found that the average velocity is positive for $H > \frac{1}{2}$, zero at $H = \frac{1}{2}$, and negative for $H < \frac{1}{2}$. For the persistent case ($H > \frac{1}{2}$), the average velocity increases monotonically with the Hurst exponent. However, for the anti-persistent case ($H < \frac{1}{2}$), there exists a value of Hurst exponent at which the average velocity takes its extremal value. When $H \rightarrow 0$, the noise term in Eq. (1) will disappear, the system is deterministic and the directed transport also disappears. When $H \rightarrow \frac{1}{2}$, the fractional Gaussian noise reduces to the white Gaussian noise, the system undergoes thermal equilibrium and the average velocity tends to zero.

IV. CONCLUDING REMARKS

In this paper, we studied the directed transport of overdamped Brownian particles driven by fractional Gaussian noises. From numerical simulations, we can find that fractional Gaussian noise can break the detailed balance and induce directed transport. Similar to the classic ratchets [1], there exists a value of noise intensity at which the average velocity takes its extremal value. The average velocity as a function of the asymmetry of the potential is

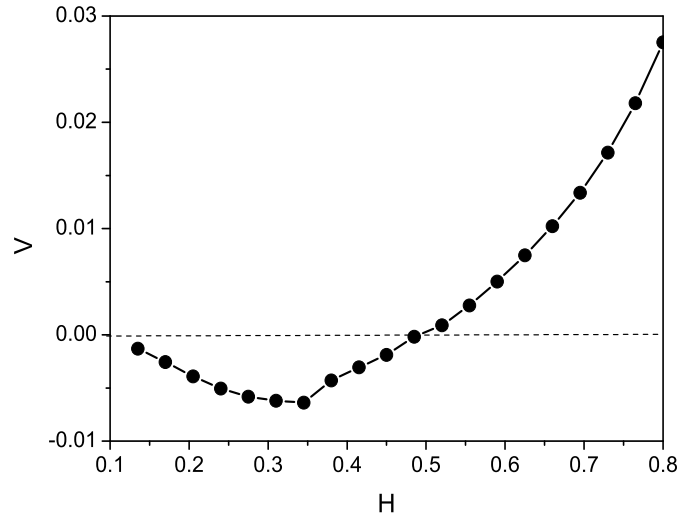


FIG. 6: Average velocity V as a function of the Hurst exponent H at $\Delta = 1.0$, $D = 0.5$, and $U_0 = 1$.

monotonic. From the numerical analysis of the spectral density of fractional Gaussian noises, it is found that the low frequency component in spectral density is larger than the high frequency component for the persistent case ($H > \frac{1}{2}$), whereas the high frequency component is dominated for the anti-persistent case ($H < \frac{1}{2}$). Due to the difference of the spectral density between the persistent and anti-persistent cases, the average velocity has the opposite sign for the two cases. Remarkably, the average velocity increases monotonically with the Hurst exponent for the persistent case. However, for anti-persistent case, there exists an optimal value of the Hurst exponent at which the velocity takes its extremal value.

Directed transport in static ratchet potentials can also be induced by the other types of noise, such as α -stable noise (Lévy ratchet)[11–14], white shot noise (shot-noise ratchet)[30], and two correlated noises (correlated ratchet)[7]. In the Lévy ratchet [11–14], the thermodynamical equilibrium is broken by the the heavy-tailed distribution of the α -stable noise. For shot-noise ratchet [30], the temporal asymmetry of white shot noise can induce an effective, inhomogeneous diffusion, so the net current occurs. In the correlated ratchet [7], fluctuation-induced transport is driven by both additive Gaussian white noise and additive colored noise. The additive colored noise can be treated as the multiplicative noise by introducing a new auxiliary variable, therefore an effective, inhomogeneous diffusion appears.

However, in our fractional Gaussian noise-induced ratchet, the directed transport is induced by the asymmetry of noise spectral density. When $H > \frac{1}{2}$, the fractional Gaussian noise contains more low frequency components, whereas the high frequency component is dominated for $H < \frac{1}{2}$.

This work was supported in part by National Natural Science Foundation of China (Grant Nos. 30600122, 11004982 and 10947166)and GuangDong Provincial Natural Science Foundation (Grant No. 06025073 and 01005249). Y. F. He also acknowledges the Research Foundation of Education Bureau of Hebei Province, China (Grant No. 2009108)

-
- [1] P. Hänggi and F. Marchesoni, *Rev. Mod. Phys.* **81**, 387 (2009).
 - [2] F. Julicher A. Adjari, and J. Prost, *Rev. Mod. Phys.* **69**, 1269 (1997).
 - [3] J. Rousselet, L. Salome, A. Adjari, and J. Prost, *Nature* **370**, 446 (1994); L. P. Faucheux, L. S. Bourdieu, P. D. Kaplan, and A. J. Libchaber, *Phys. Rev. Lett.* **74**, 1504 (1995).
 - [4] F. Marchesoni, *Phys. Rev. Lett.* **77**, 2364(1996); I. Derenyi, C. Lee, and A. L. Barabasi, *Phys. Rev. Lett.* **80**,1473 (1998); C. S. Lee et al., *Nature* **400**, 337 (1999).
 - [5] M. O. Magnasco, *Phys. Rev. Lett.* **71**, 1477 (1993); R. Bartussek, P. Hänggi, and J. G. Kissner, *Europhys. Lett.* **28**, 459 (1994).
 - [6] P. Reimann, *Phys. Rep.* **290**, 149(1997); J. D. Bao and Y. Z. Zhuo, *Phys. Lett. A* **239**, 228 (1998); B. Q. Ai, L. Q. Wang, and L. G. Liu, *Chaos, Solitons Fractals* **34**, 1265 (2007); P. Reimann, R. Bartussek, R. Haussler, and P. Hänggi, *Phys. Lett. A* **215**, 26 (1996).
 - [7] C. R. Doering, W. Horsthemke, and J. Riordan, *Phys. Rev. Lett.* **72**, 2984 (1994); R. Bartussek, P. Reimann, and P. Hänggi, *Phys. Rev. Lett.* **76**, 1166(1996).
 - [8] B. Q. Ai and L. G. Liu, *Phys. Rev. E* **74**, 051114 (2006); B. Q. Ai, *Phys. Rev. E* **80**, 011113 (2009); F. Marchesoni, S. Savel'ev, *Phys. Rev. E* **80**, 011120 (2009); B. Q. Ai, *J. Chem. Phys.* **131**, 054111 (2009).
 - [9] R. Metzler and J. Klafter, *Phys. Rep.* **339**, 1 (2000); I. Goychuk and P. Hänggi, *Phys. Rev. Lett.* **99**, 200601 (2007).
 - [10] B. Dybiec, E. Gudowska-Nowak, and I. M. Sokolov, *Phys. Rev. E* **78**, 011117 (2008); B. Dybiec, *Phys. Rev. E* **78**, 061120 (2008).
 - [11] D. Del-Castillo-Negrete, V. YU. Gonchar, and A. V. Chechkin, *Phys. Lett. A* **387**, 6693 (2008).

- [12] I. Goychuk, E. Heinsalu, M. Patriarca, G. Schmid, and P. Hänggi, Phys. Rev. E 73, 020101(R) (2006); E. Heinsalu, M. Patriarca, I. Goychuk, G. Schmid, and P. Hänggi, Phys. Rev. E 73, 046133 (2006).
- [13] J. Rosa and M. W. Beims, Physica A 386, 54 (2007).
- [14] B. Q. Ai and Y. F. He, J. Stat. Mech.: Theory Exp., P04010 (2010).
- [15] B. B. Mandelbrot and J. W. Van Ness, SIAM Rev. 10, 422 (1968).
- [16] D. Panja, J. Stat. Mech.: Theory Exp., L02001 (2010).
- [17] G. Guigas and M. Weiss, Biophys. J. 94, 90 (2008); J. Szymanski and M. Weiss, Phys. Rev. Lett. 103, 038102 (2009).
- [18] L. Lizana and T. Ambjornsson, Phys. Rev. Lett. 100, 200601 (2008).
- [19] A. Zoia, A. Rosso, and S. N. Majumdar, Phys. Rev. Lett. 102, 120602 (2009).
- [20] K. Burnecki and A. Weron, Phys. Rev. E 82, 021130 (2010); A. Weron, K. Burnecki, Sz. Mercik, and K. Weron, Phys. Rev. E 71, 016113 (2005).
- [21] I. Calvo and R. Sanchez, J. Phys. A: Math. Theor. 41, 282002 (2008); M. Bologna, F. Vanni, A. Krokhin, and P. Grigolini, Phys. Rev. E 82, 020102(R) (2010); L. Zunino, D. G. Perez, M. T. Martin, M. Garavaglia, A. Plastino, and O. A. Rosso, Phys. Lett. A 372, 4768 (2008).
- [22] T. A. Øigard, A. Hanssen, and L. L. Scharf, Phys. Rev. E 74, 031114 (2006); W. Deng and E. Barkai, Phys. Rev. E 79, 011112 (2009); J. H. Jeon and R. Metzler, Phys. Rev. E 81, 021103 (2010).
- [23] R. Garcia-Garcia, A. Rosso, and G. Schehr, Phys. Rev. E 81, 010102(R) (2010); N. Kumar, U. Harbola, and K. Lindenberg, Phys. Rev. E 82, 021101 (2010).
- [24] M. Magdziarz, A. Weron, K. Burnecki, and J. Klafter, Phys. Rev. Lett. 103, 180602 (2009); I. Eliazar and J. Klafter, Phys. Rev. E 79, 021115 (2009).
- [25] O. Y. Sliusarenko, V. Y. Gonchar, A. V. Chechkin, I. M. Sokolov, and R. Metzler, Phys. Rev. E 81, 041119, (2010); O. Y. Sliusarenko, V. Y. Gonchar, and A. V. Checkin, Urk. J. Phys. 55, 579 (2010).
- [26] S. Chaudhury and B. J. Cherayila, J. Chem. Phys. 125, 114106 (2006).
- [27] S. C. kou and X. S. Xie, Phys. Rev. Lett. 93, 180603 (2004).
- [28] A. V. Checkin and V. Y. Gonchar, Chaos, Soliton and Fractals 12, 391(2001) ; B.S. Lowen, Meth. Comput. Applied Probab. 1:4, 445 (1999).
- [29] T. Dieker, *Simulation of Fractional Brownian Motion*, Masters Thesis, Department of Math-

emtical Sciences, University of Twente, The Netherlands, 2004.

[30] J. Luczka, R. Bartussek, and P. Hänggi, *Europhys. Lett.* **31**, 431 (1995).